Synthesis of Nickel Hydroxide by Homogeneous Alkalinization. Precipitation Mechanism

Galo J. de A. A. Soler-Illia,[†] Matías Jobbágy,[†] Alberto E. Regazzoni,*[,‡] and Miguel A. Blesa[‡]

INQUIMAE, Facultad de Ciencias Exactas y Naturales, Universidad de Buenos Aires, Pabellón II, Ciudad Universitaria, 1428-Buenos Aires, Argentina, and Unidad de Actividad Química, Comisión Nacional de Energía Atómica, Av. del Libertador 8250, 1429-Buenos Aires, Argentina

Received April 19, 1999. Revised Manuscript Received July 21, 1999

Uniform microcrystalline nickel(II) hydroxide particles have been prepared via the homogeneous alkalinization of nickel(II) nitrate solutions by urea hydrolysis. The nature of the precipitated solids depends on the temperature of synthesis. At ca. 423 K, i.e., under the hydrothermal conditions attained by microwave heating, β-Ni(OH)$_2$ forms upon the fast ripening of α-Ni(OH)$_2$. In the range 363−343 K, α-Ni(OH)$_2$ is always the final product. The evolution of the systems during the precipitation of α-Ni(OH)$_2$ is analyzed in terms of the kinetic factors that control nucleation and growth. A precipitation mechanism, based on the principle of *minimal structural change*, is proposed; it is suggested that the edge-on condensation of $Ni_4(OH)_4^{4+}$ tetramers is a key step in the sequence of events that conduct from hexaaquo Ni^{2+} to α-Ni(OH)$_2$.

Introduction

Nickel (hydr)oxides are the active material of the cathodes of rechargeable alkaline batteries. As such, their electrochemical and crystallochemical properties have been thoroughly studied.[1−5] Different solid phases have been described: α- and β-Ni(OH)$_2$, with Ni in the +2 oxidation state, and β- and γ-NiOOH, with Ni in the +3 state, all of them involved in the charge−discharge cycles.[6] Among the hydroxides,[7] α-Ni(OH)$_2$ is the most active material because of its larger conductivity, which is ionic in nature.[2,3] With the aim of improving the cycling durability of Ni cathodes, attempts have been made to block the α-Ni(OH)$_2$ → β-Ni(OH)$_2$ ripening by enhancing the stability of the hydrotalcite-like α-phase.[8−10] Since the overall performance of Ni cathodes depends on the microstructural, as well as the textural, characteristics of the active material,[11] a simple and reliable synthesis procedure becomes a matter of importance.

The most commonly used precipitation procedures are indeed simple; basically, they involve the mixing of nickel salt solutions and bases. However, due to the very large supersaturations that are attained, reproducibility is seldom warranted, especially when α-Ni(OH)$_2$ is the desired product. For instance, this procedure leads to mixtures of α and β hydroxides if the precipitation reaction is not quenched rapidly.[12] The difficulties intrinsic to this procedure are further illustrated by the fact that solids described as β_{bc} (badly crystallized β-Ni(OH)$_2$)[13] and as "neither α nor β"[14] have been prepared at essentially the same synthesis conditions. To obtain single-phase α-Ni(OH)$_2$ samples, addition of surface-active solutes was found to be necessary.[15]

Homogeneous precipitation procedures, in which the degree of supersaturation is gradually increased, are more easy to control and should not face the liabilities of the aforementioned ones. Among these procedures,

[†] Universidad de Buenos Aires.
[‡] Unidad de Actividad Química.
* To whom correspondence should be addressed.

(1) Delahaye-Vidal, A.; Beaudoin, B.; Sac-Epée, N.; Tekaia-Ehlsissen, K.; Audemer, A.; Figlarz, M. *Solid State Ionics* **1996**, *84*, 239.
(2) Barnard, R.; Randell, C. F.; Tye, F. L. *J. Appl. Electrochem.* **1980**, *10*, 109.
(3) Barnard, R.; Randell, C. F.; Tye, F. L. *J. Appl. Electrochem.* **1980**, *10*, 127.
(4) Portemer, F.; Delahaye-Vidal, A.; Figlarz, M. J. *Electrochem. Soc.* **1992**, *139*, 671.
(5) Oliva, P.; Leonardi, J.; Laurent, F.; Delmas, C.; Braconnier, J. J.; Figlarz, M.; Fievet, F.; de Guibert, A. *J. Power Sources* **1982**, *8*, 229.
(6) Bode, H.; Dehmelt, K.; Witte, J. *Electrochim. Acta* **1966**, *11*, 1079.
(7) Whereas the notation β-Ni(OH)$_2$ identifies a hydroxide that is an isomorph of brucite, the notation α-Ni(OH)$_2$ has been frequently used to describe a set of compounds with chemical compositions that are more proper of basic salts rather than of a hydroxide. The latter notation, however, denotes the typical turbostratic nature of these compounds, i.e., the random orientation of the defective brucite-like Ni(OH)$_2$ layers that are spaced along the *c*-axis by intercalated water molecules. In what follows, α-Ni(OH)$_2$ identifies these hydrotalcite-like compounds without implying any specific stoichiometry.

(8) Delahaye-Vidal, A.; Figlarz, M. *J. Appl. Electrochem.* **1987**, *17*, 589.
(9) Faure, C.; Delmas, C.; Willmann, P. *J. Power Sources* **1991**, *35*, 263.
(10) Tekaia-Ehisissen, K.; Delahaye-Vidal, A.; Genin, P.; Figlarz, M.; Willmann, P. *J. Mater. Chem.* **1993**, *3*, 883.
(11) Figlarz, M.; Gérand, B.; Delahaye-Vidal, A.; Dumont, B.; Harb, F.; Coucou, A. *Solid State Ionics* **1990**, *43*, 143.
(12) Le Bihan, S.; Guenot, J.; Figlarz, M. *C. R. Acad. Sci. Paris* **1970**, *C270*, 2131.
(13) Fouassier, M.; Faure, C.; Delmas, C. *J. Power Sources* **1991**, *35*, 279.
(14) Rajamathi, M.; Subbanna, G. N.; Kamath, P. V. *J. Mater. Chem.* **1997**, *7*, 2293.
(15) Kamath, P. V.; Ismail, J.; Ahmed, M. F.; Subbanna, G. N.; Gopalakrishnan, J. *J. Mater. Chem.* **1993**, *3*, 1285.

10.1021/cm9902220 CCC: $18.00
Published on Web 10/15/1999

homogeneous alkalinization by urea hydrolysis is perhaps one of the most suitable.[16] In fact, the urea method has already been used to prepared single-phase α-Ni(OH)$_2$ powders.[17−20] The further advantages of this procedure have been nicely illustrated by Avena et al.[19] In some cases, however, $\alpha + \beta_{bc}$ mixtures have been obtained. This seems to be a consequence of the rather restricted range of experimental conditions that has been explored.

Clearly, the optimization of any synthesis procedure requires not only a systematic experimental study but also sound knowledge of the involved processes. Surprisingly, none of the previous works address the nucleation and growth mechanism. In this paper, we investigate the precipitation of nickel(II) hydroxide from urea-containing solutions under a wide range of experimental conditions, including hydrothermal conditions attained by microwave heating, and analyze the processes that lead to the formation of the solid particles.

Experimental Section

Materials. Nickel nitrate stock solutions (0.025 mol dm^{-3}) were prepared by dissolving $Ni_2(OH)_2CO_3$ in dilute HNO_3 (final pH ∼ 3), filtered through 0.22 μm pore-size cellulose nitrate membranes, and stored in plastic bottles.

All solutions were made up using analytical grade reagents and deionized water (18 MΩ cm) obtained from a Milli-Q apparatus. All glassware was washed using diluted HNO_3 (1:1 volume ratio) and rinsed thoroughly with water and steam.

Synthesis Procedures. Nickel hydroxide particles were prepared by aging solutions containing nickel nitrate (1×10^{-3} mol dm^{-3} ≤ [Ni(NO$_3$)$_2$] ≤ 5×10^{-3} mol dm^{-3}) and urea (0.5 mol dm^{-3}) at prefixed temperatures for different periods. Two series of experiments were performed. In one of them, the temperature was kept constant at 363 K and the initial nickel concentration, $[Ni(II)]_0$, varied. In the other, $[Ni(II)]_0$ was fixed at 5.4×10^{-3} mol dm^{-3} and the temperature varied between 343 and ca. 423 K. In all cases, the initial pH was fixed at 5.0 ± 0.1 by the addition of NH_3.

Experiments were performed as follows. Fresh starting solutions were prepared by mixing the necessary amounts of the Ni(II) stock solution, solid urea, and water to yield the desired reactant concentrations. Filtered aliquots (10 cm^3) were poured into 20 cm^3 screw-capped borosilicate test tubes, which were then placed in a thermostatic water bath preheated at the working temperature (±0.5 K). After prefixed time intervals, the tubes were removed from the water bath and immersed in an ice−water mixture to quench the reaction; the temperature drop during the first minute of cooling was ca. 60%.

At temperatures above 373 K, the experiments were carried out in a commercial CEM MDS 2000 microwave digestor using a 20 cm^3 heavy duty Teflon vessel. The working temperature, which should be reached in less than 3 min,[21] was estimated from the set maximum pressure using the coexistence curve of pure water.[22]

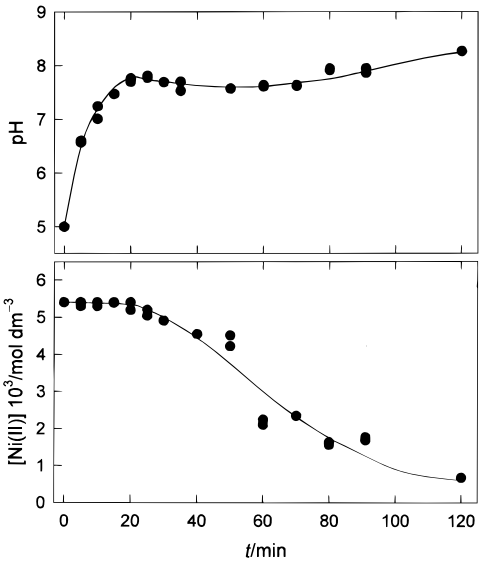

Figure 1. Time dependence of pH (upper) and Ni(II) concentration (lower) during the aging of the $[Ni(II)]_0 = 5.4 \times 10^{-3}$ mol dm^{-3} system at 363 K.

The precipitated solids were then collected by filtration through 0.22 μm pore size cellulose nitrate membranes, washed three times with cold deionized water, and dried in vacuo at room temperature. Supernatant solutions were stored for chemical analyses; pH was measured (±0.02 units) using a combined glass−electrode, and Ni(II) was determined, within 1%, by atomic absorption spectrometry (AAS).

Sample Characterization. The synthesized solids were characterized by powder X-ray diffraction (PXRD) in a Siemens D-5000 instrument, using the graphite-filtered Cu Kα radiation (λ = 1.5406 Å); peak analyses were performed with a profile fitting software.[23] All fwhm (full width at half-maximum), from which crystallite sizes were determined, were corrected for instrumental broadening using a highly crystalline quartz specimen as reference.

Scanning electron microscopy images were obtained with a Philips SEM 515 equipment. Fourier transform infrared (FTIR) spectra were recorded in a Nicolet 510 P spectrometer using KBr pellets. Elemental analyses (C, H, and N) were carried out in a Carlo Erba CHON-S analyzer. Ni contents were assessed by AAS of dissolved solids; oxygen contents were calculated by difference. TG and DSC measurements were performed at 5.0 K min^{-1}, under a nitrogen flow to prevent Ni(II) oxidation.

Results

The Evolution of the Systems. To determine the best synthesis conditions, the changes in the composition of the solutions were recorded as a function of the aging time. The evolution of pH and of dissolved Ni(II) concentration during the aging of the $[Ni(II)]_0 = 5.4 \times 10^{-3}$ mol dm^{-3} system at 363 K are shown in Figure 1. Precipitation starts once a certain critical pH value is exceeded. Soon after the precipitation onset, the pH drops as a consequence of the inversion of the unbalance of the rates of urea hydrolysis and base consumption that is prompted by the burst of nuclei.[16,24] Later, the rate of urea hydrolysis offsets that of base consumption,

(16) Soler-Illia, G. J. de A. A.; Jobbágy, M.; Candal, R. J.; Regazzoni, A. E.; Blesa, M. A. *J. Dispersion Sci. Technol.* **1998**, *19*, 207.
(17) Maruthiprasad, B. S.; Sastri, M. N.; Rajagopal, S.; Seshan, K.; Krishnamurthy, K. R.; Rao, T. S. R. *Proc. Indian Acad. Sci.* **1988**, *100*, 459.
(18) Durand-Keklikian, L.; Haq, I.; Matijevic, E. *Colloids Surf. A* **1994**, *92*, 267.
(19) Avena, M. J.; Vázquez, M. V.; Carbonio, R. E.; de Pauli, C. P.; Macagno, V. A. *J. Appl. Electrochem.* **1994**, *24*, 256.
(20) Dixit, M.; Subbanna, G. N.; Kamath, P. V. *J. Mater. Chem.* **1996**, *6*, 1429.
(21) Kingston, H. M.; Jassie, L. B. *Introduction to Microwave Sample Preparation*; ACS Professional Publications: Washington, DC, 1988.
(22) Harvey, A. H.; Peskin, A. P.; Klein, S. A. *NIST Standard Reference Database* 10; NIST/ASME Steam Properties, Ver. 2.11; USSC: Washington, DC, 1996.
(23) *Diffrac-AT* 3.0, Siemens, 1993.
(24) Candal, R. J.; Regazzoni, A. E.; Blesa, M. A. *Colloids Surf. A* **1993**, *79*, 191.

Table 1. Precipitation Onsets of α-Ni(OH)$_2$

exp no.	$[Ni(II)]_0$, 10^3/mol dm^{-3}	T/K	t^*/min	pH*	log Ω*
K902	1.50	363	15	8.08	0.53
K903	2.85	363	18	7.93	0.52
K905	4.25	363	20	7.88	0.59
S590	5.40	363	22	7.81	0.56
S580	5.40	353	45	7.68	0.30
S570	5.40	343	160	7.83	0.59
S5M	5.40	ca. 423	<5		

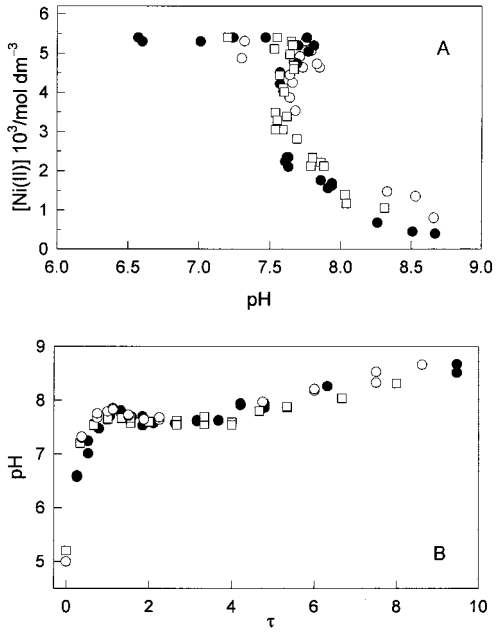

Figure 2. Evolution of dissolved Ni(II) concentration (A) and pH (B) during the aging of the $[Ni(II)]_0 = 5.4 \times 10^{-3}$ mol dm^{-3} system at 343 (○), 353 (□), and 363 K (●). (A) presents the pH dependence of [Ni(II)]. In (B), pH is plotted as a function of the reduced time ($\tau = t/t^*$).

and a well-defined pH plateau accompanies massive precipitation.

Table 1 shows that the pH values at the precipitation onsets, pH*, although fairly independent of temperature, depend on the initial Ni(II) concentration. Instead, Ω*, the derived supersaturations (calculated as IAP*/Kps, where IAP* is the ion activity product at the precipitation onset and Kps is the solubility product of nickel hydroxide, which was taken from ref 25), are constant and independent of the synthesis conditions (Table 1); the only exception is experiment S580. Thus, $\Omega^* = 10^{0.56\pm0.05}$ can be identified as the critical supersaturation.

Figure 2a shows the changes of the dissolved Ni(II) concentration at three different temperatures, plotted as a function of the measured pH. At a fixed $[Ni(II)]_0$, the extent of precipitation is solely determined by the evolution of pH, irrespective of the synthesis temperature. The observed right-leaned hump reflects again the faster rate of base consumption (compared to that of urea hydrolysis) caused by the burst of nuclei. The observed overlap further suggests that the overall shape of the pH evolution is also independent of temperature, although in different time scales. Figure 2b shows the course followed by pH at the different temperatures,

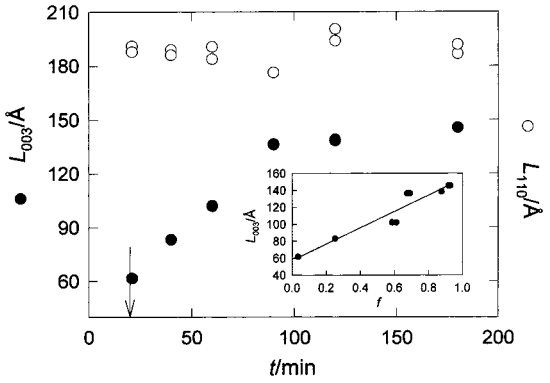

Figure 3. Evolution of the crystallite size during the precipitation of α-Ni(OH)$_2$ from the $[Ni(II)]_0 = 5.4 \times 10^{-3}$ mol dm^{-3} system at 363 K; the arrow indicates the onset of precipitation. Inset: crystallite height plotted as a function of the precipitated fraction.

presented as a function of the reduced time, $\tau = t/t^*$, where t^*, also listed in Table 1, is the time required to reach the precipitation onset. The curves overlap each other. The *master* curves presented in Figure 2 indicate that, once the temperature dependence of t^* has been established, the aging time required to reach a certain precipitation extent can be estimated from just a reference experiment. Further, they convey the idea that the same overall precipitation mechanism operates under the different synthesis conditions.

PXRD patterns of the solids precipitated during the aging of the $[Ni(II)]_0 = 5.4 \times 10^{-3}$ mol dm^{-3} system at 363 K show peaks, which gain in definition as the aging progresses, at 7.25, 3.614, 2.657, and 1.552 Å; they correspond to the [003], [006], [012], and [110] reflections of α-Ni(OH)$_2$, respectively.[26] Figure 3 depicts the evolution of the size of the crystallites along the [003] and [110] directions. It shows that the growth is highly anisotropic; note the almost instantaneous development of the basal planes, which is followed by a much slower growth along the *c*-direction. The height of the crystallites, L_{003}, levels off once most of the Ni(II) has been removed from solution; the inset in Figure 3 shows that L_{003} increases almost linearly with the fraction of precipitated Ni(II). Figure 3 further indicates that a crystalline, albeit turbostratic, solid forms as soon as the precipitation is triggered.

Crystallite sizes presented in Figure 3 were calculated using the Warren modification of the Scherrer equation,

$$B_{hkl}(2\theta) = \frac{K\lambda}{L_{hkl}\cos\theta} \qquad (1)$$

where B_{hkl} is the fwhm of a given [hkl] peak, L_{hkl} is the crystallite size along the [hkl] direction, and K is the structure factor, which takes into account the strong asymmetry of the [hk0] reflections that is produced by the turbostraticity of α-Ni(OH)$_2$; for the [hk0] reflections, $K = 1.84$, and for the [00l] ones, $K = 0.94$.[27]

Synthesis of α-Ni(OH)$_2$. PXRD patterns of samples synthesized under different experimental conditions are presented in Figure 4. At 363 K and below, α-Ni(OH)$_2$

(25) Novak-Adamic, D.; Kosovic, B. *J. Inorg. Nucl. Chem.* **1973**, *35*, 2371.

(26) Braconnier, J. J.; Delmas, C.; Fouassier, M.; Figlarz, M.; Beaudouin, B.; Hagenmueller, P. *Rev. Chim. Miner.* **1984**, *21*, 496.

(27) Klug, H. P.; Alexander, L. E. *X-Ray Diffraction Procedures*, 2nd ed.; Wiley: New York, 1974.

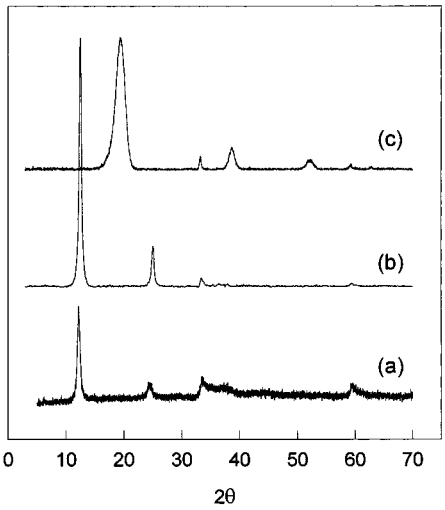

Figure 4. PXRD patterns of powders obtained upon the aging of the $[Ni(II)]_0 = 5.4 \times 10^{-3}$ mol dm^{-3} system at different conditions: (a) 180 min at 343 K; (b) 5 min at ca. 423 K; (c) 30 min at ca. 423 K.

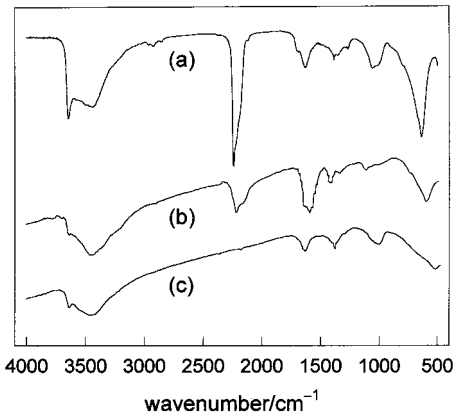

Figure 5. FTIR spectra of powders obtained upon the aging of the $[Ni(II)]_0 = 5.4 \times 10^{-3}$ mol dm^{-3} system at different conditions: (a) 180 min at 343 K; (b) 5 min at ca. 423 K; (c) 30 min at ca. 423 K.

is always the final product; at ca. 423 K, instead, the initially formed α-$Ni(OH)_2$ (pattern b) evolves to β-$Ni(OH)_2$ (pattern c) in a rather short period (30 min). The lattice parameters of the synthesized α-$Ni(OH)_2$ particles are $a = 3.103$ Å and $c = 21.75$ Å. The latter, derived from the measured interbasal distance ($d_{003} = 7.25$ Å), is in good agreement with those reported earlier for α-$Ni(OH)_2$ particles precipitated from urea-containing solutions[18,20] but is somewhat lower than those reported for α-$Ni(OH)_2$ particles prepared using other precipitation procedures.[1,5] The final sizes of the α-$Ni(OH)_2$ crystallites range from 150 to 200 Å.

Figure 5 presents the FTIR spectra of the different samples. Spectra a and b are typical of α-$Ni(OH)_2$ particles prepared by the urea method.[18,20] The narrow band at 3650 cm^{-1} corresponds to the ν_{O-H} stretching of the geminal OH groups of the brucite-like structure. The broad band centered at 3400 cm^{-1} is due to the ν_{O-H} vibration of H-bonded water molecules located in the interlamellar space of the turbostratic structure of α-$Ni(OH)_2$. The very strong absorption band at 2250 cm^{-1} is assigned to the $\nu_{C\equiv N}$ vibration of OCN^- anions,[28] and those at 1600 and 1430 cm^{-1} are assigned to the $\nu_{C=O}$ doublet of bidentate and monodentate carbonate ions in C_s symmetry.[29] The band at 680 cm^{-1} corresponds to the δ_{O-H} wagging vibration.[5]

The bands of cyanate (2250 cm^{-1}) and carbonate (1600 and 1430 cm^{-1}) denote the incorporation of the byproducts of urea hydrolysis within the solid particles. Incorporation of carbonate is a characteristic of most of the solids synthesized via the urea method; actually, in many cases, the final product is a basic carbonate.[16,30,31] Incorporation of cyanate, however, is rare and has been reported only in the case of nickel hydroxide.[17,18,20] The reason for this distinct behavior may be traced back to the comparatively high pH at which nickel hydroxide precipitates (cf. ref 32) and to the rather inert nature of the d^8 Ni^{2+} ions; as pH rises, the hydrolysis of urea slows down and the steady-state concentration of cyanate increases considerably,[16] thus favoring the likely incorporation of robust $NiOCN^+$ complexes into the growing $Ni(OH)_2$ sheets. Elemental analyses of typical samples are in the order 4.7% N, 5.8% C, 2.0% H, and 51.0% Ni and yield the formula $Ni(OH)_{1.27}(CO_3)_{0.17}(OCN)_{0.39}\cdot 0.46H_2O$, which is in good agreement with earlier results.[17]

Undoubtedly, OCN^- and CO_3^{2-} replace lattice OH^- ions or, in the words of Delahaye-Vidal et al.,[1] take up OH vacancies. These anions cannot be electrostatically intercalated within the interlamellar space of α-$Ni(OH)_2$, for such an intercalation is only akin to LDHs (layered double hydroxides), the "positive" counterpart of clays.[33,34] It has been suggested,[35] however, that the protonation of basal OH groups may provide the required excess of positive charge. This possibility is indeed unlikely, because among the different types of surface OH groups, tricoordinated OH_2 is the most acidic one.[36]

Nickel hydroxide particles prepared by other common procedures, say, dropwise addition of ammonia to Ni(II) nitrate solutions, present a somewhat lower degree of OH substitution and yield, typically, $Ni(OH)_{1.43}(CO_3)_{0.19}(NO_3)_{0.19}\cdot 1.8H_2O$.[1] They also present larger water contents, which are reflected in their larger d_{003} spacings that may be up to 8.5 Å. Such spacings correspond to the thickness of a poorly packed water layer separating the octahedral $Ni(OH)_2$ sheets.[5] The lower interbasal distances characterizing the α-$Ni(OH)_2$ particles prepared by the urea method, on the other hand, are consistent with interlamellar heights that correspond to a loose water monolayer.[37] The origin of

(28) Forster, D.; Goodgame, D. M. L. *J. Chem. Soc.* **1965**, 262.
(29) Nakamoto, K. *Infrared and Raman Spectra of Inorganic and Coordination Compounds*, 4th ed.; Wiley: New York, 1986; p 220.
(30) Candal, R. J.; Regazzoni, A. E.; Blesa, M. A. *J. Mater. Chem.* **1992**, *2*, 657.
(31) Soler-Illia, G. J. de A. A.; Candal, R. J.; Regazzoni, A. E.; Blesa, M. A. *Chem. Mater.* **1997**, *9*, 184.
(32) (a) Baes, C. F.; Mesmer, P. E. *The Hydrolysis of Cations*; John Wiley: New York, 1976. (b) Smith, R. M.; Martell, A. E. *Critical Stability Constants*; Plenum: New York, 1989; Vol. 6.
(33) Brindley, G. W.; Kikkawa, S. *Am. Mineral.* **1979**, *64*, 836.
(34) LDHs have the formula $M(II)_{1-x}M(III)_x(OH)_2X_{x/n}\cdot yH_2O$, where n is the charge number of the exchangeable anion X. See, e.g.: Constantino, V.; Pinnavaia, T. J. *Inorg. Chem.* **1995**, *34*, 883.
(35) Kamath, P. V.; Annal-Therese, G. H.; Gopalakrishnan, J. *J. Solid State Chem.* **1997**, *128*, 38.
(36) (a) Hiemstra, T.; van Riemsdijk, W. H.; Bolt, G. H. *J. Colloid Interface Sci.* **1989**, *133*, 91. (b) Hiemstra, T.; de Wit, J. C. M.; van Riemsdijk, W. H. *J. Colloid Interface Sci.* **1989**, *133*, 105. (c) Hiemstra, T.; van Riemsdijk, W. H. *Colloids Surf.* **1991**, *59*, 7.
(37) Le Bihan, S.; Figlarz, M. *Thermochim. Acta* **1973**, *6*, 319.

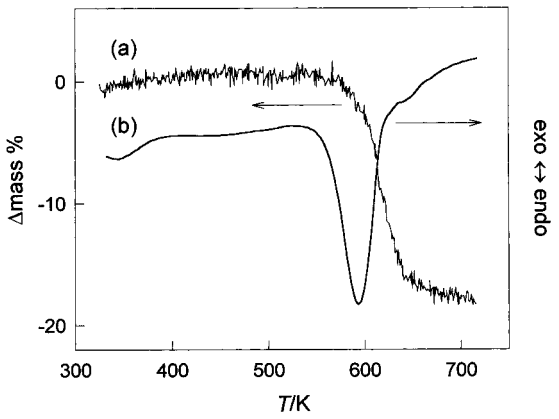

Figure 6. TG (a) and DSC (b) of α-$Ni(OH)_2$ obtained by aging the $[Ni(II)]_0 = 5.4 \times 10^{-3}$ mol dm^{-3} system at 343 K for 180 min. Temperature ramp, 5 K min^{-1}; N_2 flow, 50 cm^3 min^{-1}; the sample was vacuum-dried before TG analysis.

this singular disparity is unclear and cannot be attributed to any possible effect due to the presence of cyanate. Perhaps, this disparity would reflect a subtle difference in the growth mechanisms operating under the different synthesis conditions.

The different water contents of the α-$Ni(OH)_2$ samples prepared by the different procedures are further reflected in their overall thermal behaviors. Figure 6 indicates that the thermal decomposition of α-$Ni(OH)_{1.27}(CO_3)_{0.17}(OCN)_{0.39}\cdot 0.46H_2O$ to NiO (*bunsenite*) takes place in a single endothermic step centered at 593 K (DSC), in which interlamellar and condensation water molecules, as well as carbonate and cyanate decomposition products, are released simultaneously (TGA); the shallow band centered at ca. 373 K (DSC) corresponds to the loss of physisorbed water. In the case of samples with larger water contents, instead, formation of NiO is preceded by the partial loss of interlamellar water molecules that takes place within 393−433 K;[37] this partial dehydration leads to water contents of about 0.6 molecules per nickel and is followed by a reduction of the interbasal distance to ca. 7.0 Å. These different thermal behaviors should indicate the larger interaction between the interlamellar water molecules and the octahedral $Ni(OH)_2$ sheets in the monolayer configuration. Interestingly, the presence of cyanate in the α-$Ni(OH)_2$ particles synthesized by the urea method does not affect the temperature at which NiO forms.[18−20,37,38]

The SEM micrograph presented in Figure 7 shows the typical morphology of the synthesized α-$Ni(OH)_2$ particles. Although they exhibit the expected crystalline habit, their petal-like shape denotes a certain degree of unordered crystallite aggregation; note that the average particle size is much larger than the nominal size of the crystallites. While the common α-$Ni(OH)_2$ preparation procedures seem to provide conditions under which aggregation is minimized (small hexagonal platelets usually form), the mild conditions of the urea method favor the formation of crystalline aggregates.[16] In fact, spherical aggregates of α-$Ni(OH)_2$ have been prepared via the urea method, albeit under different experimental conditions.[18]

(38) Gabr, R. M.; El-Naimi, A. N.; Al-Thani, M. G. *Thermochim. Acta* **1992**, *197*, 307.

Figure 7. SEM micrograph of α-$Ni(OH)_2$ particles synthesized by aging the $[Ni(II)]_0 = 5.4 \times 10^{-3}$ mol dm^{-3} system at 343 K for 180 min.

Synthesis of *β*-$Ni(OH)_2$. As shown in Figure 4 (pattern c), the urea method is also suitable for the synthesis of *β*-$Ni(OH)_2$. In this case, however, hydrothermal conditions are required; in fact, at 363 K, no *β*-$Ni(OH)_2$ could be detected, even when the systems were aged for up to 96 h. The lattice parameters of the formed *β*-$Ni(OH)_2$ particles are $a = 3.119$ Å and $c = 4.560$ Å, and as judged from the FTIR results (see spectrum c in Figure 5), they are cyanate-free and contain only a modest amount of carbonate. Morphologically, the particles resemble those of α-$Ni(OH)_2$ (cf. Figure 7).

Although the characteristics of the synthesized *β*-$Ni(OH)_2$ particles are roughly the same of those prepared by prolonged boiling of highly alkaline α-$Ni(OH)_2$ suspensions,[1,5] the hydrothermal aging of nickel nitrate solutions containing urea has clear advantages: the synthesis is rapid and involves a single operation. Indeed, at ca. 423 K, an aging period of just 30 min suffices to produce pure *β*-$Ni(OH)_2$ powders.

Discussion

This work shows that once the adequate experimental conditions have been set, the urea method is a very suitable procedure for the synthesis of single-phase α-$Ni(OH)_2$ and *β*-$Ni(OH)_2$ powders. Although the relatively high contents of cyanate of the α-$Ni(OH)_2$ powders prepared by this method may constitute an important liability of the material, our results demonstrate that the presence of cyanate does not affect its crystallochemical properties (Figure 4) or its thermal ones (Figure 6); furthermore, the electrochemical response of $\alpha + \beta_{bc}$ samples seems not to be affected by the presence of cyanate.[19]

The precipitation of nickel hydroxide from urea-containing solutions can be rationalized interpreting the Ostwald step rule[39] in terms of the principle of *minimal structural change*;[40,41] this implies that the coordinative environment of the aqueous species that promote nucle-

(39) Ostwald, W. *Z. Phys. Chem.* **1897**, *22*, 289.

(40) Hückel, W. *Theoretische Grundlagen der Organischen Chemie*; Akademische Verlagsgellschaft: Leipzig, 1934.

(41) Boldyreva, E. In *Implications of Molecular and Material Structure for New Technologies*; Howard, J. A. K., Allen, F. H., Shields, G. P., Eds.; NATO-ASI Series E; Kluwer Academic Press: Dordretch, 1999; p 151.

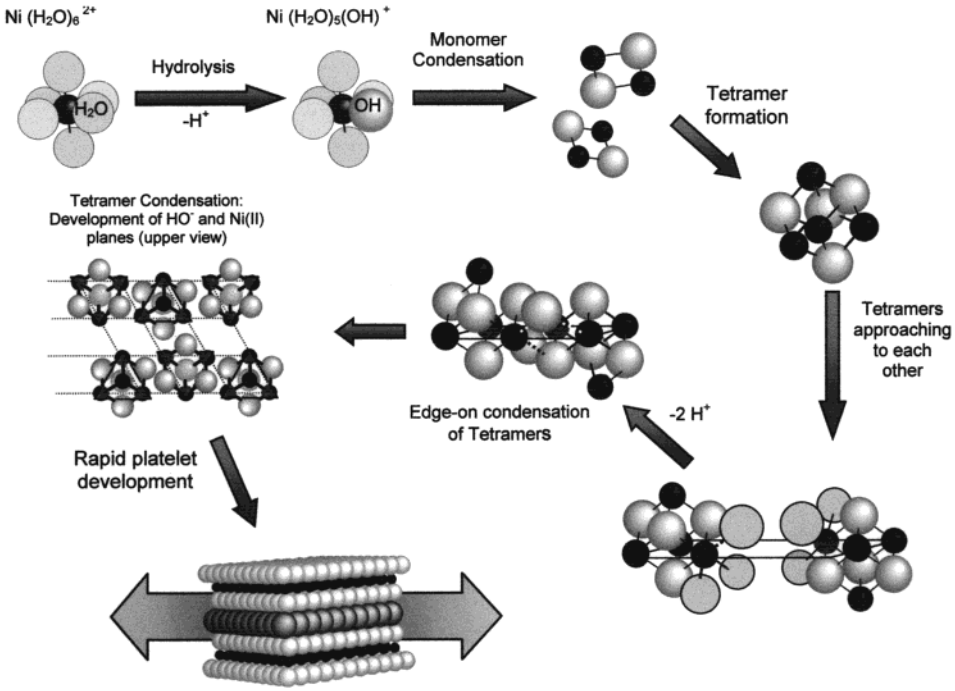

Figure 8. Schematic representation of the sequence of events that lead to the nucleation of α-$Ni(OH)_2$.

ation should closely resemble those of the ions in the solid state. As urea hydrolyzes,

$$OC(NH_2)_2 \underset{k_{-1}}{\overset{k_1}{\rightleftharpoons}} OCN^- + NH_4^+ \qquad (2)$$

$$OCN^- + H^+ + 2H_2O \xrightarrow{k_2} HCO_3^- + NH_4^+ \qquad (3)$$

different nickel hydroxo species form along with cyanate and bicarbonate complexes. At the precipitation onset (say, pH 7.81), the hexaaquo Ni^{2+} ion predominates, $NiOH^+$, $NiOCN^+$, $Ni(OCN)_2^0$, and $NiHCO_3^+$ accounting for about 1, 10, 1, and 3%, respectively;[42] $Ni_2(OH)_2^{2+}$ and $Ni_4(OH)_4^{4+}$ are negligible. Yet, the constancy of Ω* (Table 1) indicates that only OH^- ions participate in nuclei formation. Since nucleation of metal (hydrous)-oxides is often preceded by the formation of oligomeric hydroxo moieties,[43,44] the role of the polynuclear species should be central, especially that of $Ni_4(OH)_4^{4+}$, in which OH^- ions are already tricoordinated.[45,46] Thus, we propose that the nucleation of α-$Ni(OH)_2$ is driven by the edge-on condensation of tetrameric units (see the scheme presented in Figure 8); a similar nucleation mechanism has already been postulated for monoclinic ZrO_2.[47] This process is the continuation of the olation reactions that lead to the dimer and to the tetramer, which are assumed to be stages of a smooth sequence that conducts to the solid and not dead-end entities. Condensation along the Ni_3 plane of the tetramers leads to

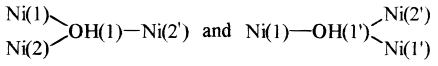

bonds (the prime denotes ions of a different tetramer), where the bridging OH^- ions lose their coordination to the out-of-plane Ni(4); formation of Ni(1)−OH−Ni(1′) and Ni(2)−OH−Ni(2′) bonds and release of two H_3O^+ take place simultaneously. Aggregation of additional tetramers defines the close-packed arrangement of OH^- ions and reduces the number of bonds linking the out-of-plane Ni(4) ions, which, at a certain point, are ejected from the growing polyion. Once the size of the polyion surpasses a critical value, subsequent growth proceeds by incorporation of hydroxylated and complexed monomers.

This bidimensional condensation model, in line with the periodic bond chain (PBC) approach,[48] leads to single $Ni(OH)_2$ layers, which must serve as templates for the condensation of further tetramers that triggers the nucleation and growth of the next layers in a turbostratic fashion. Accordingly, the crystallites identified at almost the precipitation onset (Figure 3) are composed of seven $Ni(OH)_2$ layers with a basal dimension of ca. 19 nm, i.e., about 35 × 35 unit cells. Although other nucleation pathways can be envisaged, all of them invoke aqueous Ni(II) species that have not been described in the literature.

As the aging proceeds, further growth in the *c*-direction takes place (Figure 3). The linear relationship between L_{003} and the fraction of precipitated nickel (see inset in Figure 3) suggests that the number of crystal-

(42) The distribution of aqueous Ni(II) species was calculated solving eqs 2 and 3 under the assumption that all hydrolytic and complexation reactions involving Ni(II) are equilibrated; kinetic data and equilibrium constants were taken from refs 16 and 32, respectively. For further details, see: Soler-Illia, G. J. de A. A. Ph.D. Thesis, Universidad de Buenos Aires, Argentina, 1998.

(43) Matijević, E. *Pure Appl. Chem.* **1980**, *52*, 1179.
(44) Livage, J.; Henry, M.; Sanchez, C. *Prog. Solid State Chem.* **1988**, *18*, 259.
(45) Kolski, G. B.; Kjeldahl, N. K.; Margerum, D. W. *Inorg. Chem.* **1969**, *8*, 1211.

(46) It should be recalled that in the brucite-like $Ni(OH)_2$ layers each OH^- ion is tricoordinated to Ni^{2+} ions that occupy one-half of the octahedral holes of the hexagonal close packing of hydroxide ions.

(47) Bleier, A.; Cannon, R. M. *Mater. Res. Soc. Symp. Proc.* **1986**, *73*, 71.
(48) Hartman, P. In *Crystal Growth: an Introduction*; Hartman, P., Ed.; North-Holland: Amsterdam, 1973.

lites remains constant after the burst of nuclei; viz., nucleation and particle growth occur separately. This is a consequence of the fast relief of the supersaturation that occurs soon after the precipitation onset (see Figure 2). The growth of the *xy*-planes, on the other hand, is rapidly arrested; L_{110} remains constant during the entire aging (Figure 3). This is probably due to a blocking action by CO_3^{2-} or, more likely, OCN^-; the poisoning of growth sites by anions is well-known.[49] The size of the final polycrystalline petal-like particles (Figure 7) is, however, determined by the extent of the ordered aggregation of crystallites (primary particles) along the basal direction, in line, again, with the PBC approach; ordered aggregation of primary particles is well documented.[50,51] This process may be assisted by carbonate anions, which can not only reduce the charge of the edges of the "flat" crystallites but also bridge them tightly.

Under hydrothermal conditions (423 K), the initially precipitated α-$Ni(OH)_2$ readily ripens into β-$Ni(OH)_2$ (Figure 4). This result is another example of the well-known Ostwald step rule. According to Le Bihan and Figlarz[52] and Delahaye-Vidal et al.,[1] this transformation proceeds through a dissolution−recrystallization mechanism, despite the similarities of the crystal structures. Although the factual evidence is scarce, the absence of cyanate in the final solids (Figure 5, spectrum c) supports this contention. Crystallization of β-$Ni(OH)_2$ should follow essentially the same precipitation sequence outlined above.

Acknowledgment. This work was partially supported by grants from UBA (EX036) and CONICET (PIP 4196). G.J. de A.A.S.-I. thanks the Fellowship awarded by UBA. A.E.R. and M.A.B. are members of CONICET. Thanks are due to Grupo Análisis de Trazas, INQUIMAE, for sharing their microwave digestor. The authors are grateful to Gabbo's, where rendezvous were sparkling, indeed.

CM9902220

(49) Sunagawa, I. *Estudios Geolog.* **1982**, *38*, 127.
(50) Hsu, W. P.; Ronnquist, L.; Matijević, E. *Langmuir* **1988**, *4*, 31.
(51) Ocaña, M.; Matijević, E. *J. Mater. Res.* **1990**, *5*, 1083.
(52) Le Bihan, S.; Figlarz, M. *J. Cryst. Growth* **1972**, *13/14*, 458.